



## Dissolved iron in the vicinity of the Crozet Islands, Southern Ocean

Hélène Planquette<sup>a,\*</sup>, Peter J. Statham<sup>a</sup>, Gary R. Fones<sup>b</sup>, Matthew A. Charette<sup>c</sup>,  
C. Mark Moore<sup>d</sup>, Ian Salter<sup>a</sup>, Florence H. Nédélec<sup>a</sup>, Sarah L. Taylor<sup>a</sup>, M. French<sup>e</sup>,  
A.R. Baker<sup>e</sup>, N. Mahowald<sup>f</sup>, T.D. Jickells<sup>e</sup>

<sup>a</sup>National Oceanography Centre, University of Southampton, Southampton SO17 3ZH, UK

<sup>b</sup>School of Earth and Environmental Sciences, University of Portsmouth, Burnaby Building, Burnaby Road, Portsmouth PO1 3QL, UK

<sup>c</sup>Woods Hole Oceanographic Institution, Woods Hole, MA 02543, USA

<sup>d</sup>University of Essex, Colchester CO4 3SQ, UK

<sup>e</sup>School of Environmental Sciences, University of East Anglia, Norwich NR4 7TJ, UK

<sup>f</sup>National Centre for Atmospheric Research, P.O. Box 3000, Boulder, CO 80307, USA

Received 17 October 2006; received in revised form 30 March 2007; accepted 26 June 2007

### Abstract

The annual phytoplankton bloom occurring north of the Crozet Plateau provides a rare opportunity to examine the hypothesis that natural iron fertilization can alleviate high-nutrient low-chlorophyll (HNLC) conditions normally associated with the Southern Ocean. Therefore, during CROZet natural iron bloom and EXport experiment (CROZEX), a large multidisciplinary study performed between November 2004 and January 2005, measurements of total dissolved iron ( $D_{\text{Fe}} \leq 0.2 \mu\text{m}$ ) were made on seawater from around the islands and atmospheric iron deposition estimated from rain and aerosol samples.

$D_{\text{Fe}}$  concentrations were determined by flow injection analysis with *N,N*-dimethyl-*p*-phenylenediamine dihydrochloride (DPD) catalytic spectrophotometric detection.  $D_{\text{Fe}}$  concentrations varied between 0.086 and 2.48 nM, with low values in surface waters. Enrichment of dissolved iron ( $> 1 \text{ nM}$ ) at close proximity to the islands suggests that the plateau and the associated sediments are a source of iron. Waters farther north also appear to be affected by this input of coastal and shelf origin, although dissolved iron concentrations decrease as a function of distance to the north of the plateau with a gradient of  $\sim 0.07 \text{ nM km}^{-1}$  at the time of sampling. Using lateral and vertical diffusion coefficients derived from Ra isotope profiles and also estimates of atmospheric inputs, it was then possible to estimate a  $D_{\text{Fe}}$  concentration of  $\sim 0.55 \text{ nM}$  to the north of the islands prior to the bloom event, which is sufficient to initiate the bloom, the lateral island source being the largest component. A similar situation is observed for other Sub-Antarctic Islands such as Kerguelen, South Georgia, that supply dissolved iron to their surrounding waters, thus enhancing chlorophyll concentrations.

© 2007 Elsevier Ltd. All rights reserved.

**Keywords:** Dissolved iron, Crozet Islands, Southern Ocean, HNLC

### 1. Introduction

The hypothesis that iron (Fe) can act as a limiting micro-nutrient in high-nutrient low-chlorophyll

\*Corresponding author.

E-mail address: [hfp@noc.soton.ac.uk](mailto:hfp@noc.soton.ac.uk) (H. Planquette).

(HNLC hereafter) regions is now generally accepted and has been investigated on a number of occasions (Boyd et al., 2000, 2007; de Baar et al., 2005). The Fe hypothesis originally proposed by Martin (1990) has led to numerous studies that all demonstrate that the addition of Fe to HNLC waters causes an increase in phytoplankton productivity. Subsequent investigations into Fe's role in phytoplankton physiology also have revealed important findings. Among them, one can cite its role in photosynthetic and respiratory electron transport, nitrate reduction, and chlorophyll synthesis (Sunda and Huntsman, 1995, 1997). The broader implication is that in HNLC waters, the presence of Fe can increase the efficiency of the biological pump and promote drawdown of atmospheric carbon dioxide (CO<sub>2</sub>) (Bakker et al., 2001, 2005; Boyd et al., 2004; Law et al., 2006; Martin, 1990).

The Southern Ocean is subjected to these HNLC conditions and is depicted as the largest potential sink of anthropogenic CO<sub>2</sub> in the global ocean (Martin, 1990; Tréguer and Pondaven, 2001) and as a key system in the context of climate change (Sarmiento et al., 1998). However, due to the existence of distinct regional sub-systems differing in their physical and biological properties (Arrigo et al., 1998; Tréguer and Jacques, 1992), this ocean should not be viewed as one entity.

There have been numerous scientific investigations conducted over the last decade to try and understand the relationship between Fe and the biogeochemical functioning of HNLC regions. Recently, several *in situ* Fe-enrichment experiments in the Southern Ocean (e.g., SOIREE (Bakker et al., 2005; Boyd et al., 2000), SOFEX (Buesseler et al., 2004; Coale et al., 2004), EISENEX (Boyé et al., 2005; Croot et al., 2005)), that are summarized by de Baar et al. (2005) and Boyd et al. (2007), have highlighted the importance of Fe availability for phytoplankton communities in this region. However, as pointed out by Chisholm (2000), such artificial enrichments cannot represent natural processes effectively, since the perturbation could lead to many unintended side effects such as changing the structure of the marine ecosystem, or generating greenhouse gases other than CO<sub>2</sub>.

Most Fe inputs to the remote global surface waters are derived from aeolian dust, with the largest sources (e.g., Saharan desert) being in the northern hemisphere (Sarhou et al., 2003). However, such atmospheric inputs are estimated to be small in the Southern Ocean (Jickells et al., 2005) although very few data exist for this region.

Sites of natural and continuous fertilization of Fe do exist where there is permanent interaction between water masses and margins of landmasses; this phenomenon is generally called “the island mass effect”. Several previous studies (Croot et al., 2004a; de Baar et al., 1999; de Jong et al., 1998; Löscher, 1999; Sarhou et al., 1997) have inferred Fe-fertilized phytoplankton blooms around island systems in the Southern Ocean such as South Georgia (Korb et al., 2004; Moore and Abbott, 2002), Kerguelen (Blain et al., 2001, 2002, 2007; Bucciarelli et al., 2001), Bouvet (Croot et al., 2004a) and the Crozet Islands (Metzl et al., 1999; Sedwick et al., 2002).

Therefore, the two-leg CROZet natural Fe bloom and EXport experiment (CROZEX) cruise on *RRS Discovery* in the austral summer of 2004/2005 in the waters surrounding the Crozet Islands provided an excellent opportunity to examine how the natural sources of Fe, originating either from the islands directly or from the relatively shallow surrounding sediments, could relieve Fe stress and therefore promote phytoplankton growth, particularly by the larger cells typically responsible for the export of particulate carbon and nitrogen.

Within the Sub-Antarctic region of the Southern Ocean, between the Polar and Subtropical water masses, the volcanic Crozet archipelago located on a shallow plateau on the eastern flank of the southwest Indian Ocean ridge comprises two main islands in the east and three smaller islands 100 km to the west. The Crozet area exhibits high concentrations of chlorophyll during austral spring and summer (Fiala et al., 2003) to the north of the islands, and is particularly suited to a study of Fe distributions, because of the way in which the topography and the zonal winds constrain the local circulation patterns and the extent of the bloom (Pollard and Read, 2001; Pollard et al., 2002).

In the present paper, new data on dissolved Fe ( $D_{Fe} \leq 0.2 \mu\text{m}$ ) distributions around the Crozet Islands are presented. Particular emphasis has been placed on the sources of Fe to the upper water column, and on the different processes that drive the distribution of Fe, such as biological uptake, mixing with deeper waters, advection of Fe-rich waters from the islands and atmospheric inputs.

## 2. Sampling and methods

### 2.1. Study area

Seawater and atmospheric samples were collected during the CROZEX cruises (D285 and D286) on

board *RRS Discovery* between 3 November 2004 and 21 January 2005. The research area was located around the Îles Crozet (45°95' and 46°50'S, 50°33' and 52°58'E), which are the surface projections of the Crozet Plateau (~1220 km × ~600 km) situated approximately 2000 km south east of South Africa on the edge of the Southern Ocean. Stations were established for water sampling and physical observations at strategic points in areas to the north-west, north-east, in close proximity and directly south of the two main islands, Île de la Possession and Île de l'Est. The stations sampled and their positions are shown in Fig. 1 and Table 1. Station M3 was sampled several times, providing an opportunity to assess the temporal evolution of conditions at one site.

## 2.2. Sampling and cleaning procedures

### 2.2.1. Chlorophyll-*a*

Samples for chlorophyll-*a* (Chl *a*) analysis (100–200 mL) were filtered onto Whatman GF/F filters then extracted into 90% acetone for 24 h in a dark refrigerator before measurement on a Turner designs fluorometer (Welschmeyer, 1994).

### 2.2.2. $D_{Fe}$

Prior to the cruise, storage sample bottles were soaked in ~2% (v/v) aqueous Decon detergent for 3 days and subsequently soaked for 3 days each in 50% HCl (v/v) and 50% (v/v) HNO<sub>3</sub> (Fisher Scientific). In between steps, the bottles were rinsed with Milli-Q water. After removal from the acid bath, the sample bottles were rinsed with sub-boiled distilled water. The sample bottles were filled with Milli-Q water acidified with quartz sub-boiling distilled HCl (Q-HCl) and stored in clean zipper seal polyethylene bags in a class-100 clean-air laboratory. Polycarbonate filters were soaked for 2 weeks in 10% v/v Q-HCl, rinsed and stored in sub-boiled distilled water.

Water-column samples were collected with a trace-metal clean Titanium CTD (conductivity, temperature, depth) rosette system in 10-L Ocean Technical Equipment (OTE) bottles modified for trace metal sampling and processed on board in a container equipped with a class 100 laminar flow bench. After pressurizing the OTE bottles with filtered high-purity nitrogen (BOC Gases), the valves were opened and seawater was directed through an acid-washed 0.2- $\mu$ m polycarbonate filter

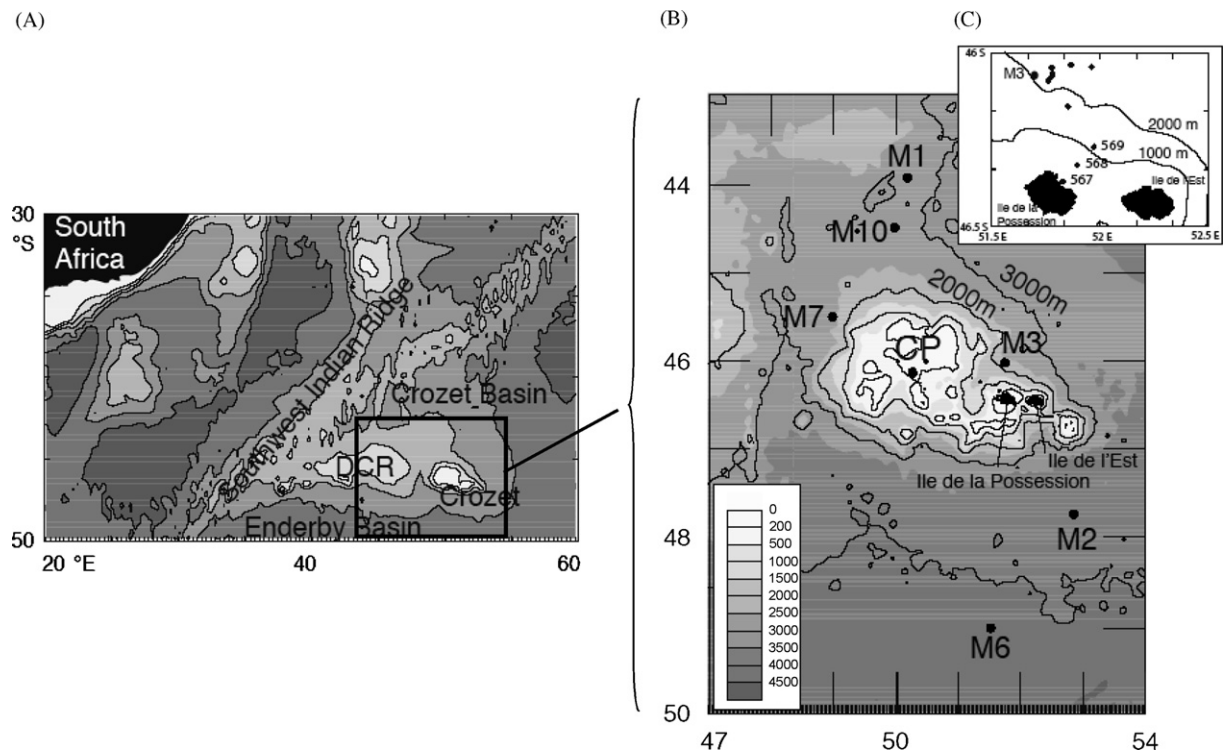


Fig. 1. (A) Location of the Crozet Islands relative to South Africa. (B) Stations sampled for  $D_{Fe}$  during D285 and D286 North and South of the Crozet plateau. (C) Detail of stations between Baie Américaine (567) on Île de la Possession and M3.

Table 1

Station locations, depth, dissolved iron concentrations ( $<0.2 \mu\text{m}$ ), temperature, salinity, density, and Chl *a* concentrations during D285 and D286

Station details	Depth (m)	$D_{\text{Fe}}$ (nM)	Temperature ( $^{\circ}\text{C}$ )	Salinity	Density ( $\sigma_0$ )	Chl <i>a</i> ( $\text{mg m}^{-3}$ )
M1 (491)	5	0.22	5.813	33.727	26.566	0.90
11/11/2004	10	–	5.803	33.727	26.566	0.76
43.92049°S	20	0.31	5.802	33.727	26.566	0.79
50.26742°E	40	–	5.801	33.727	26.567	0.77
3118 m	50	0.34	5.761	33.726	26.570	–
	60	–	5.769	33.727	26.571	0.73
	70	–	5.746	33.730	26.576	0.76
	110	0.38	4.417	33.890	26.882	–
	250	0.30	3.135	34.085	27.117	–
	500	0.29	2.741	34.301	27.347	–
M3.1 (496)	5	–	4.368	33.828	26.822	0.61
13/11/2004	10	–	4.371	33.829	26.822	0.87
46.06809°S	15	0.10	4.370	33.829	26.822	0.68
51.78529°E	42	0.09	4.227	33.828	26.839	1.1
2287 m	65	–	3.752	33.828	26.839	1.03
	175	0.09	3.125	33.876	26.938	–
	218	0.10	2.990	33.856	26.981	–
	300	0.12	2.858	34.008	27.114	–
M2.1 (502)	5	0.27	3.279	33.793	26.871	0.34
19/11/2004	10	0.24	3.155	33.787	26.881	0.39
47.79537°S	20	–	3.174	33.790	26.890	0.35
52.86216°E	40	0.24	3.159	33.791	26.903	0.42
3870 m	60	(4.38) <sup>a</sup>	3.160	33.801	26.912	0.43
	80	0.22	3.161	33.805	26.914	0.43
M6.1 (511)	5	–	2.710	33.794	26.948	0.27
22/11/2004	10	0.20	2.687	33.794	26.948	0.25
49.00557°S	20	–	2.705	33.809	26.960	0.25
51.50046°E	40	0.25	2.530	33.811	26.966	0.45
4275 m	60	–	2.572	33.812	26.974	0.27
	80	0.21	2.469	33.820	26.976	0.38
	250	0.40	1.661	33.911	27.129	–
M3.3 (516)	5	–	4.368	33.842	26.826	0.47
25/11/2004	10	–	4.370	33.842	26.826	0.48
46.05961°S	20	(2.08) <sup>a</sup>	4.369	33.842	26.826	0.49
51.79093°E	40	0.19	4.227	33.841	26.841	0.49
3986 m	60	(0.40)	3.875	33.862	26.894	0.49
	80	0.28	3.621	33.872	26.928	0.41
M7 (524)	5	–	5.530	33.816	26.675	1.34
27/11/04	10	(1.65) <sup>a</sup>	5.533	33.816	26.675	1.34
45.49943°S	15	(0.63)	5.533	33.816	26.675	1.39
49.00242°E	25	(0.73)	5.533	33.817	26.675	1.41
2749 m	35	0.29	5.528	33.818	26.677	1.38
	55	0.27	5.044	33.837	26.748	1.22
	75	0.44	3.897	33.897	26.920	–
	100	0.34	3.444	33.906	26.971	–
	125	0.23	3.132	33.921	27.013	–
	150	0.46	3.008	33.939	27.038	–
	200	0.20	2.969	34.016	27.103	–
	300	0.26	2.872	34.143	27.214	–
	400	0.46	2.706	34.223	27.293	–
	500	0.23	2.650	34.294	27.355	–

Table 1 (continued)

Station details	Depth (m)	$D_{Fe}$ (nM)	Temperature (°C)	Salinity	Density ( $\sigma_t$ )	Chl $a$ ( $mg\ m^{-3}$ )
M10.1 (563)	5	0.48	6.126	33.786	26.578	0.80
21/12/2004	10	–	6.132	33.786	26.577	0.73
44.52528°S	15	0.40	6.142	33.786	26.576	–
49.96059°E	25	–	6.125	33.786	26.578	0.8
2943 m	35	0.31	5.998	33.787	26.595	0.81
	55	–	5.432	33.790	26.666	–
	75	0.30	4.459	33.806	26.789	0.20
	125	0.16	3.700	33.902	26.943	–
	200	0.30	3.195	34.007	27.075	0.037
BA (567)	5	1.05	4.563	33.871	26.830	0.57
22/12/2004	25	0.68	4.520	33.872	26.834	0.56
46.36854°S	50	2.16	4.370	33.883	26.863	0.54
51.82754°E	80	1.13	4.248	33.889	26.874	0.47
83 m						
BA + 1 (568)	5	0.60	4.633	33.870	26.819	0.60
22/12/2004	25	0.52	4.644	33.870	26.819	0.62
46.32332°S	50	0.56	4.605	33.870	26.823	0.62
51.89459°E	100	0.39	3.956	33.908	26.924	0.27
379 m	200	1.01	3.435	33.982	27.034	0.30
	300	2.08	2.986	34.075	27.151	0.19
	376	0.56	2.760	34.190	27.262	0.06
BA + 2 (569)	5	0.16	4.662	33.855	26.796	0.88
22/12/2004	25	0.15	4.678	33.864	26.810	1.00
46.26997°S	50	0.32	4.049	33.898	26.899	0.45
51.97083°E	100	0.15	3.669	33.962	27.007	0.18
1491 m	300	0.42	2.803	34.112	27.199	0.04
	750	0.29	2.606	34.438	27.476	–
M3.4 (572)	5	(1.71) <sup>a</sup>	5.211	33.826	26.720	1.01
22/12/2004	10	–	5.211	33.831	26.725	0.948
46.06223°S	15	–	5.211	33.831	26.725	1.01
51.78169°E	25	0.26	5.211	33.831	26.725	0.95
2375 m	35	0.38	5.212	33.831	26.725	0.97
	55	–	4.960	33.835	26.756	0.82
	75	0.26	4.427	33.852	26.829	–
	175	0.31	3.108	33.931	27.023	–
	500	0.22	2.614	34.243	27.316	–
M3.5 (592)	5	0.24	5.039	33.807	26.725	0.61
31/12/2004	10	–	5.027	33.826	26.741	0.62
46.05134°S	15	–	5.022	33.832	26.747	0.72
51.77591°E	25	0.27	4.992	33.848	26.763	0.78
2404 m	35	–	4.914	33.851	26.774	0.73
	55	0.12	4.773	33.857	26.795	0.79
	100	0.41	3.912	33.915	26.933	–
	200	0.15	3.022	34.010	27.094	–
M2.2 (605)	10	(0.52)	5.043	33.764	26.690	0.26
06/01/2005	20	–	5.041	33.764	26.691	0.30
47.80111°S	40	–	4.843	33.765	26.714	0.32
52.84952°E	50	0.09	4.809	33.766	26.719	–
3883 m	60	–	4.681	33.767	26.734	0.43
	80	–	4.212	33.773	26.789	0.72
	100	0.16	3.719	33.783	26.846	0.35
	150	–	2.488	33.844	27.008	0.13
	160	0.17	2.349	33.855	27.027	–
	200	0.11	2.035	33.910	27.097	–

Table 1 (continued)

Station details	Depth (m)	$D_{Fe}$ (nM)	Temperature (°C)	Salinity	Density ( $\sigma_0$ )	Chl <i>a</i> (mg m <sup>-3</sup> )
M3.7 (622)	5	0.15	6.075	33.831	26.619	4.94
10/01/2005	10	–	6.075	33.831	26.620	5.10
46.03412°S	20	0.23	6.075	33.831	26.619	4.95
51.86656°E	40	–	5.661	33.838	26.705	3.94
2322 m	50	–	4.742	33.871	26.833	0.88
	60	–	4.288	33.897	26.889	–
	80	0.10	3.881	33.925	26.945	0.29
	100	–	3.711	33.961	27.006	–
	150	0.09	3.313	33.997	27.057	–
	200	–	3.002	34.056	27.133	–
	300	0.34	2.742	34.117	27.205	–
	400	–	2.700	34.187	27.264	–
	500	0.20	2.641	34.270	27.337	–

A dash indicates that no sample was collected; (a) denotes the sample was grossly contaminated from OTE bottle; ( ) denotes the sample is thought to be contaminated from the ship by a specific comparison with the rest of the profile. It is suggested that for future projects, CTD sampling should not be conducted so close to the stationary or slowing ship (<30 m).

housed in a Teflon filtration unit. Clean low-density polyethylene bottles (1 L, 500 mL, Nalgene) were used to store samples after being rinsed twice with the seawater sample. After collection, samples were acidified to pH 1.7 with Q-HCl and stored for at least 2 months prior to analysis.

### 2.3. Analysis of total dissolved iron in seawater samples

#### 2.3.1. Apparatus

Total dissolved Fe concentrations ( $D_{Fe}$  hereafter) were measured in acidified (pH 1.7) seawater samples, using flow injection analysis (FIA) with in-line preconcentration and spectrophotometric detection (Lohan et al., 2006; Measures et al., 1995). This method is based on the in-line preconcentration of Fe(III) on a nitriloacetic acid (NTA, Quiagen) resin, placed in a Global FIA 2-cm mini-column. Eluted Fe(III) then catalyzes the oxidation of *N,N*-dimethyl-*p*-phenylenediamine dihydrochloride (DPD, Sigma-Aldrich) by hydrogen peroxide (H<sub>2</sub>O<sub>2</sub>, Trace metal Grade, Fisher Scientific). It is assumed that all Fe(II) is oxidized to Fe(III) by the addition of H<sub>2</sub>O<sub>2</sub> to a final concentration of 10 μM in the sample prior to the DPD oxidation step.

The manifold (Fig. 2) consisted of a 8-channel peristaltic pump (Gilson) with PharMed<sup>®</sup> tubes (Cole Palmer) of various internal diameters to obtain the appropriate flow rates. A 6-port valve (VICI, Valco instruments) was used in two different positions: loading/rinsing and eluting. All connect-

ing tubing used was 0.8 mm internal diameter Teflon. The buffer/DPD and the rinsing solutions were cleaned in-line using 2 × 1 cm Global-FIA mini-columns packed with NTA Superflow resin. The pH of the solution stream was maintained at pH 5.6 with an ammonium acetate buffer, prepared with ammonium acetate crystals obtained by bubbling filtered high-purity gaseous ammonia (BOC) through sub-boiled distilled acetic acid in an ice bath. To minimize contamination, sample and reagent bottles were positioned within a class-100 laminar flow bench. Prior to analysis, the entire manifold was rinsed for 2 h with 1.5 N Q-HCl. Hydrogen peroxide solution (5%) and DPD solution (0.05 M) were prepared daily.

Absorbance was measured using a UNICAM 7825 spectrophotometer fitted with a 1-cm flow through cell. The entire system, including signal acquisition and data processing, was controlled by a Lab-VIEW (version 7.2, National Instruments Corp.) programme. The time for one analytical cycle was approximately 15 min and a minimum of two replicate analyses per sample were made.

#### 2.3.2. Calibration and performance

The instrument was calibrated daily by analyzing acidified (pH 1.7) low-Fe seawater samples from the study area that had been spiked with a diluted Fe(III) standard solution (SPEX plasma standard). Standard additions were typically in the range 0.1–0.8 nM. Results were calculated from integration of the peak areas. Replicate analyses ( $n = 2–3$ ) were performed for all samples and standard

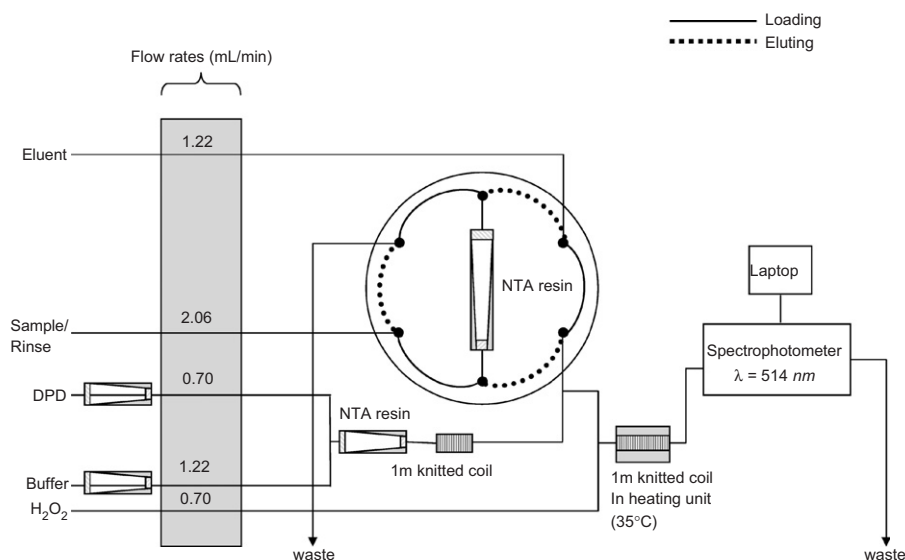


Fig. 2. FIA manifold used for the pre-concentration and determination of iron in seawater.

Table 2  
Aerosol sample collection details during D286 and non-sea-salt Ca (nss Ca) and soluble Si concentrations

Event	Start date	Start position	Volume collected (mL)	Fe concentration (nmol L <sup>-1</sup> )
CRO-R2	08/11/2004	40.63°S, 41.98°E	60	187
CRO-R3	08/11/2004	40.95°S, 43.37°E	100	6
CRO-R4	09/11/2004	41.25°S, 44.69°E	520	56
CRO-R5	18/11/2004	46.06°S, 51.79°E	250	288
CRO-R6	22/11/2004	49°S, 51.50°E	200	50
CRO-R7	30/11/2004	44.95°S, 49.94°E	130	121
CRO-R9	03/12/2004	43.12°S, 47.19°E	130	1858

solutions. Blank values varied between 0.058 and 0.09 nM, with a mean of  $0.073 \pm 0.016$  nM and the detection limit was 0.048 nM. NASS-5 ( $3.71 \pm 0.63$  nM; our value:  $3.67 \pm 0.18$  nM) and the reference seawater from the recent Fe intercomparison exercise (Sampling and Analysis of Fe (SAFe) SAFe deep ( $0.91 \pm 0.09$  nM; our value:  $0.95 \pm 0.11$  nM) seawaters taken in the North Pacific at 1000 m were used for the validation of the technique and values obtained fell within the quoted ranges. As our samples were acidified for a long period of time, the risk of bias caused by a fraction of the Fe being unavailable to the resin is low as confirmed by Lohan et al. (2006) using the same technique.

#### 2.4. Atmospheric sampling and analysis

Atmospheric sampling (Table 2) was conducted on the deck above the bridge, the highest on the ship

and well forward of ship emission sources. Samples were only collected when wind and ship movements guaranteed no contamination from the ship itself. Rainwater samples (Table 3) were collected for trace metal analysis as described previously (Spokes et al., 2001) using a clean polypropylene 40-cm diameter funnel attached to a clean LDPE sample bottle. Samples were frozen immediately after collection until return to the laboratory. Before analysis by inductively coupled plasma optical emission spectroscopy (ICP-OES), defrosted samples were acidified with concentrated HNO<sub>3</sub> (Aristar, BDH) to an amount equivalent to 1 mL L<sup>-1</sup> of sample (pH < 2) for at least 2 weeks and hence represent an estimate of total wet deposition. Aerosols were collected using a high-volume (1 m<sup>3</sup> min<sup>-1</sup>) air sampler (Graseby-Anderson) onto cellulose (Whatman 41) 25 × 20-cm collection substrates. One-quarter of each filter was extracted in ultrapure water using

Table 3

Fe concentrations and deposition fluxes obtained from the rain samples collected during D285

Sample	Start date and time (UTC)	Start position	End date time (UTC)	End position (m <sup>3</sup> )	Air volume (nmol m <sup>-3</sup> )	nss Ca (nmol m <sup>-3</sup> )	Si
CRO I 01	15/12/2004 11:00	37.47°S, 34.31°E	18/12/2004 08:43	42.50°S, 42.46°E	4049.0	0.5	0.015
CRO I 02	19/12/2004 10:58	43.07°S, 47.15°E	21/12/2004 11:10	44.77°S, 50.51°E	4497.6	2.6	0.081
CRO I 04	25/12/2004 06:55	45.94°S, 56.51°E	27/12/2004 06:55	46.00°S, 56.15°E	2897.6	0.2	0.017
CRO I 05	29/12/2004 07:10	46.00°S, 55.11°E	31/12/2004 07:35	46.06°S, 51.78°E	3027.3	0	0.015
CRO I 07	04/01/2005 07:10	49.00°S, 51.33°E	06/01/ 2005 07:45	48.23 °S, 52.28°E	3004.6	0	0.011
CRO I 08	06/01/2005 07:45	48.30°S, 52.18°E	08/01/2005 07:30	46.41°S, 51.91°E	3190.7	0	0.022

1 h of ultrasonic agitation and major ions determined by ion chromatography (Jickells et al., 2003). A separate quarter was similarly extracted with 1 mM NaHCO<sub>3</sub> buffer (pH 7) for determination of soluble Si (Baker et al., 2006a). Throughout the sampling and analyses, appropriate blank and quality control procedures were used (Spokes et al., 2001; Baker et al., 2006a).

Air parcel back trajectories (Draxler and Rolph, 2003) for all rain and aerosol sampling periods show air masses had no contact with any land masses apart from Antarctica for at least the 5 days prior to collection, and hence we were sampling truly remote Southern Ocean air.

### 3. Results

Salinity, temperature, Chl *a* and Fe concentrations are reported in Table 1.

#### 3.1. Hydrography, Chl *a* and macronutrients

##### 3.1.1. Hydrography

Large-scale and mesoscale circulation is described in detail by Pollard et al. (2007) and Read et al. (2007) and summarized in Fig. 3. Briefly, the

topography of the plateau (Park et al., 2002; Pollard and Read, 2001) significantly influences the general circulation. HNLC water masses of the Sub-Antarctic Front (SAF) intrude northwards to the west of Crozet, and are retroflected eastwards at 42°S. As a consequence, the area to the north (42°S–46°S) of the Crozet Plateau is semi-enclosed, and water that has been in contact with the Plateau is rarely transported south as indicated by trajectories of Argo profiling Floats (Pollard et al., 2007). Consequently, the spatially large bloom observed in this HNLC area is clearly constrained to the north and west by the SAF, which separates it from higher Chl *a* concentrations farther north associated with the Sub-Tropical Front and the Agulhas Return Current.

##### 3.1.2. Chl *a* and nutrients

Satellite imagery based on MODIS and SeaWiFS data (Venables et al., 2007) demonstrates that the peak of the bloom occurred prior to our arrival. Commencing in mid-September, the bloom was constrained mainly to the north of the islands, bounded by the SAF, with Chl *a* concentrations reaching a local maximum of 8 μg L<sup>-1</sup> at the beginning of November (Venables et al., 2007).



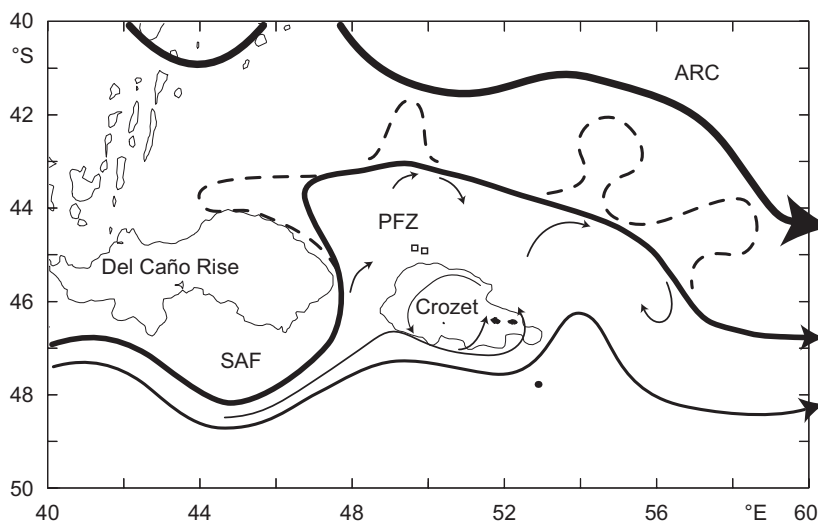


Fig. 3. Main features of circulation around the Crozet Plateau, taken from Pollard et al. (2007). ARC: Agulhas Return Current. PFZ: Polar Frontal Zone. SAF: Sub-Antarctic Front.

The bloom declined by the end of November, and surface Chl *a* values reached their lowest concentrations,  $0.6 \mu\text{g L}^{-1}$ , with a maximum of  $1.4 \mu\text{g L}^{-1}$  close to the islands. However, in late January, further blooms were observed north of the islands.

Nitrate concentrations decreased from  $24 \mu\text{M}$  south to  $18 \mu\text{M}$  north of the plateau over the sampling period, and initial silicate concentrations of  $18.5 \mu\text{M}$  became almost totally depleted ( $0.2 \mu\text{M}$ ) in the region to the north of the plateau by mid-January (Sanders et al., 2007).

Phytoplankton productivity for the region followed the same general pattern as for Chl *a* distribution (Seeyave et al., 2007). Low rates ( $<0.5 \text{gC m}^{-2} \text{d}^{-1}$ ) were measured at Stations M2 and M6 to the south of the islands in HNLC waters, and  $\sim 3 \text{gC m}^{-2} \text{d}^{-1}$  was measured at the M3 site just to the north of the islands during the bloom in January.

### 3.2. Atmospheric inputs

#### 3.2.1. Dry deposition

Aerosol samples were not specifically collected for trace metals due to sampling constraints, so we inferred atmospheric dust deposition flux ( $F_{\text{dust}}$ ) using two approaches. Firstly, we used excess (non-sea-salt), aerosol calcium (nss Ca hereafter) and assumed this was associated with crustal dust (Ca content of dust  $A_{\text{Ca}} = 1.6 \text{wt}\%$ , assuming excess Ca is 100% soluble (Croot et al., 2004b),

Table 4  
Estimated terrestrial dust fluxes to the region

Analyte	Concentration ( $\text{nmol m}^{-3}$ )	Deposition flux ( $\text{nmol m}^{-2} \text{d}^{-1}$ )
$\text{NO}_3^-$	$1.0 \pm 0.3$	1730
$\text{NH}_4^+$	$3.6 \pm 0.9$	320
nss $\text{Ca}^{2+}$	$0.1 \pm 0.2^*$	$172^*$
	$0.55 \pm 1$	
$\text{Sol}_{\text{Si}}$	$0.016 \pm 0.004^*$	$28^*$
	$0.027 \pm 0.027$	

$n = 6$  except  $*n = 5$ , one apparently anomalous result excluded.

RAM = relative atomic mass):

$$F_{\text{dust}} = \frac{F_{\text{nss Ca}} \text{RAM}_{\text{Ca}}}{A_{\text{Ca}}} \quad (1)$$

Secondly, we used estimates of aerosol soluble Si, which we assumed to be entirely of terrestrial origin (an upper limit since seawater Si may have contributed significantly), with an assumed Si solubility ( $\text{Sol}_{\text{Si}}$ ) of 0.3% (Baker et al., 2006a) and assuming the abundance of Si in ( $A_{\text{Si}}$ ) dust to be 30 wt%

$$F_{\text{dust}} = \frac{F_{\text{Si}} \text{RAM}_{\text{Si}}}{A_{\text{Si}} \text{Sol}_{\text{Si}}} \quad (2)$$

Deposition fluxes ( $F$ ) were calculated from atmospheric concentrations (Table 4) assuming nitrate, excess Ca and silicate are associated with coarse-mode aerosol and ammonium with fine mode and using deposition velocities of 2 and  $0.1 \text{cm s}^{-1}$ , respectively,

for the two modes (Baker et al., 2003). Atmospheric N deposition estimates are provided for the sake of completeness; given residual N is available in seawater throughout the season in this region, this supply from the atmosphere is not needed to support productivity.

These two approaches, using calcium and silica, gave broadly similar results (0.16 and 0.32 g dust m<sup>-2</sup> yr<sup>-1</sup>, respectively), and we therefore used a dust flux of 0.2 g m<sup>-2</sup> yr<sup>-1</sup>, which is the average of the two estimates rounded to one decimal place. This dust flux corresponds to a dry deposition flux of Fe of 127 μmol m<sup>-2</sup> yr<sup>-1</sup>, assuming dust to be 3.5% Fe (see Section 4.2 for uncertainties).

### 3.2.2. Wet deposition

Wet deposition of Fe ( $F_w$ ) was estimated using  $F_w = C P$ , where  $C$  is the volume weighted mean concentration of Fe in the rain samples (excluding CRO-R9, which was contaminated) and  $P$  is the precipitation rate for the region.  $C$  was calculated from the Fe concentration ( $C_i$ ) and volume ( $V_i$ ) of each sample using

$$C = \frac{\sum C_i V_i}{\sum V_i}. \quad (3)$$

Estimating precipitation rate in this oceanic region is complicated by orographic rainfall on the islands, and no data appear to be available for Crozet. Taljaard and Loom (1984) quote precipitation estimates for the two nearest islands (Marion and Kerguelen) as 2499 and 1117 mm yr<sup>-1</sup>, respectively, so we averaged these and assumed a precipitation of 1808 mm yr<sup>-1</sup>. Some precipitation may fall as snow and may scavenge dust differently from rain, but we have no quantitative information with which to address this, so chose to apply this precipitation rate to the rain samples collected. This translates to a wet deposition rate for total Fe of 198 μmol m<sup>-2</sup> yr<sup>-1</sup>. The total Fe deposition is thus calculated at 325 μmol m<sup>-2</sup> yr<sup>-1</sup> with 61% of this occurring as wet deposition. Uncertainties in these fluxes are considered in Section 4.2. Southern Ocean dust and Fe flux estimates from field campaigns are very limited, but the fluxes here are substantially lower than those of Gaiero et al. (2003) from Patagonia and comparable to those seen in the very high rainfall regions of coastal South Island, New Zealand (Halstead et al., 2000). Average rainwater Fe concentrations from Halstead et al. (2000) and Croot et al. (2005) are similar to those reported here.

### 3.3. Dissolved iron

Vertical profiles of  $D_{Fe}$  are shown in Figs. 4–6, and detailed in Table 1. The profiles are grouped together for three broad locations: an oligotrophic control area south of the plateau (Station M6 [511]; Fig. 4A, Station M2 [502] and [605]; Fig. 4B and C), Station M3 northeast of the plateau (Fig. 5), and Baie Américaine (BA) stations in close proximity to the plateau (569, 568, 567; Figs. 6A–C). With the exception of Baie Américaine stations,  $D_{Fe}$  concentrations for all vertical profiles are characteristically low (<1 nM), ranging from ~0.1 to 0.5 nM. The inshore stations of Baie Américaine are characterized by generally higher  $D_{Fe}$  concentrations, with maxima of ~2 nM at 50 m (Station 567, Fig. 6A) and 300 m (Station 568, Fig. 6B), respectively. Typically, we observe some  $D_{Fe}$  depletion in surface waters, while below the surface mixed layer (usually ~80 m, Venables et al., 2007),  $D_{Fe}$  concentrations were higher.

#### 3.3.1. Southern sites (M6 and M2)

Station M6 (511, Fig. 4A) is located south of the islands in HNLC water masses that are not believed to be influenced by the plateau (Fig. 3, Pollard et al., 2007). Surface-water temperatures were close to 2 °C and the constant density down to ~125 m implies deep mixing. Consequently,  $D_{Fe}$  concentrations above this depth exhibit little variability (range 0.21–0.25 nM) while Chl *a* concentrations are also low (0.18–0.26 μg L<sup>-1</sup>), both typical of Southern Ocean HNLC regions (Sedwick et al., 2002). However, below the pycnocline, there is a  $D_{Fe}$  maximum value of 0.4 nM at 250 m depth.

Station M2 (502, Fig. 4B and 605, Fig. 4C) is located northeast of M6. Surface-water temperatures varied from 3.3 and 5 °C. Between mid-November (4B) and early January (4C), Chl *a* values varied between 0.26 and 0.35 μg L<sup>-1</sup>, whilst  $D_{Fe}$  decreased from 0.22 to 0.09 nM during this period in the top 100 m. This decrease corresponds to a small bloom (Venables et al., 2007) that occurred in late December, with the phytoplankton community presumably removing the available Fe.

Overall, these values are consistent with this being a typical HNLC region in contrast to the north of the plateau.

#### 3.3.2. Station M3

M3 (Station 496; Fig. 5A, Station 572 Fig. 5B; Station 592 Fig. 5C, Station 622, Fig. 5D) is located

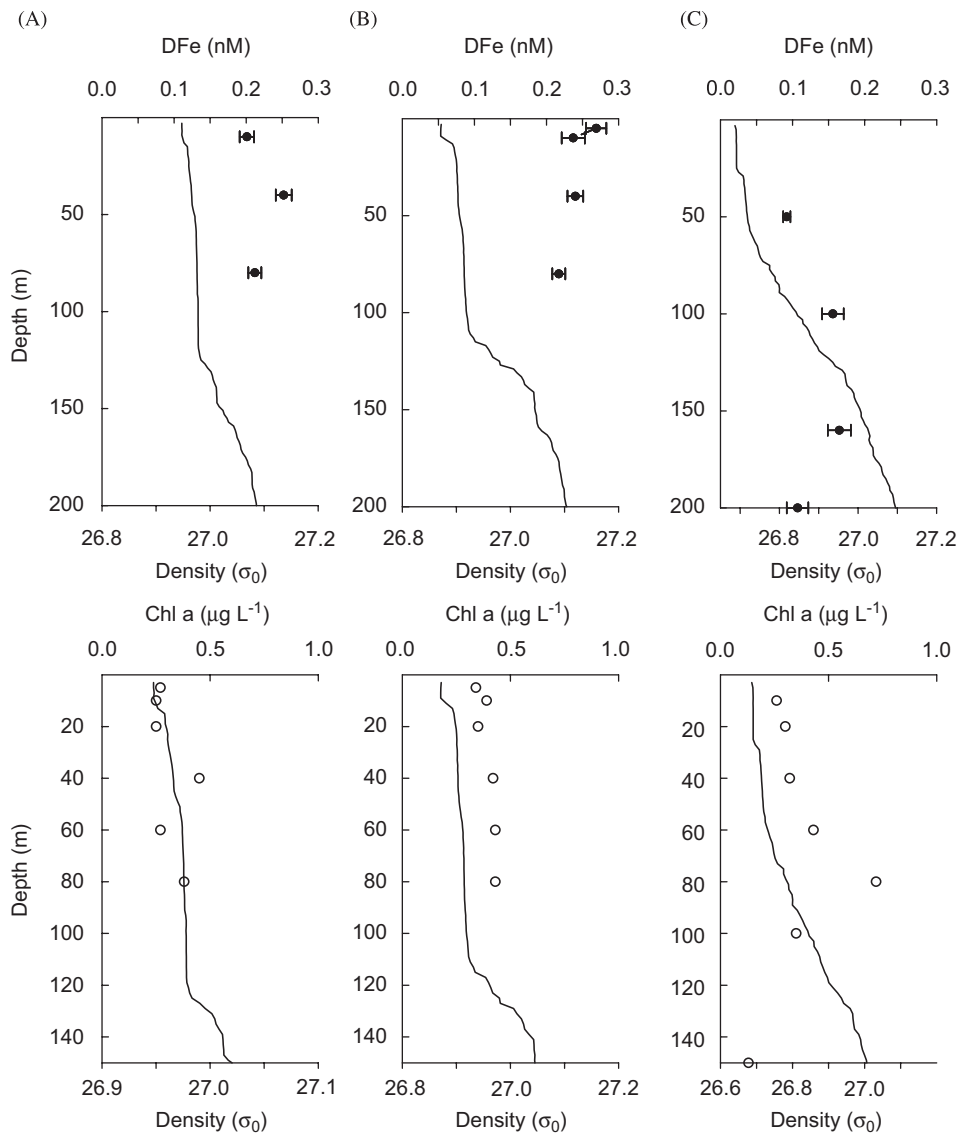


Fig. 4. Water-column profiles of  $D_{Fe}$ , salinity, temperature and Chlorophyll  $a$  at: (A) M6, Station 511 (22/11/2004); (B) M2.1, Station 502 (19/11/2004) and (C) M2.2, Station 605 (06/01/2005).

~35 km north of the plateau in an area where it was hypothesized that the bloom developed in direct response to an input of dissolved Fe from the islands. This station was occupied five times. Only four stations are shown on Fig. 5 as too few data were available for Station 516 (Table 1). Sea-surface temperature varied from 4.4 °C at the beginning of the sampling period (13/11/2004, Station 496) to 6.1 °C at the end (Station 622). The mixed-layer depths were relatively shallow (40–70 m) for all the occupations.

The first occupation (496, Fig. 5A) was after the main bloom event (Venables et al., 2007) in mid-October and appeared to be under the influence of

an influx of new water coming from the HNLC south (Pollard et al., 2007). Consequently, surface chlorophyll concentrations were lower than expected at this station, with a maximum of 0.15  $\mu\text{g L}^{-1}$  at 42 m depth.  $D_{Fe}$  concentrations above the mixed-layer depth were very low with a mean value of 0.1 nM. The later two occupations (Stations 572 (Fig. 5B) and 592 (Fig. 5C)) exhibit low chlorophyll concentrations, varying from 0.58 to 0.85  $\mu\text{g L}^{-1}$ . In parallel,  $D_{Fe}$  concentrations in the upper water column varied with time, and had a mean value of 0.26 nM within the mixed layer. At Station 592, a  $D_{Fe}$  maximum of 0.4 nM was

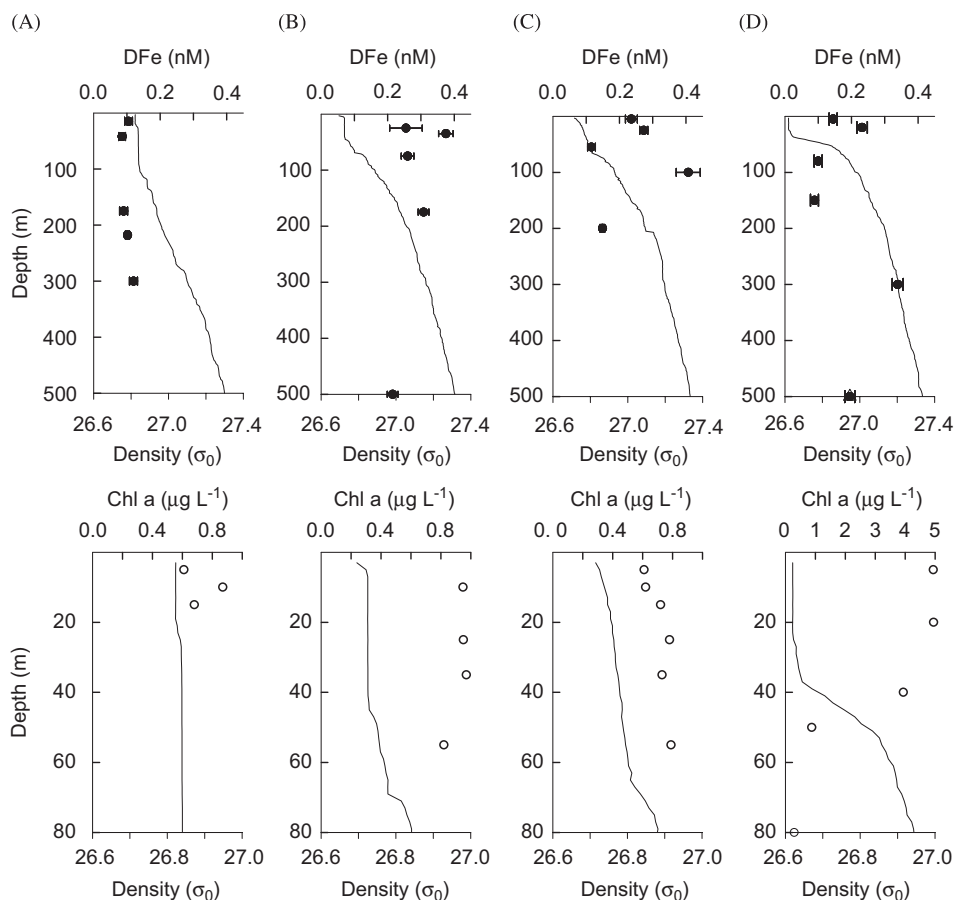


Fig. 5. Water column profiles of  $D_{Fe}$ , salinity, temperature and Chlorophyll *a* at M3: (A) Station 496 (13/11/2004); (B) Station 572 (22/12/2004); (C) Station 592 (31/12/2004) and (D) Station 622 (10/01/2005).

observed just below the pycnocline. The last occupation in January 2005 (Station 622, Fig. 5D) was during a secondary bloom event, with chl *a* concentrations reaching  $5\ \mu g\ L^{-1}$ , with  $D_{Fe}$  concentrations depleted down to  $0.1\ nM$  within the mixed layer. Another  $D_{Fe}$  maximum of  $0.34\ nM$  was observed at 300 m. No values as high were found at the Southern sites.

### 3.3.3. Baie Américaine

Three stations were occupied: 567 (Fig. 6A), 568 (Fig. 6B), and 569 (Fig. 6C), which were located progressively further away from the shore. Station 567 was approximately 1 km from the shore, in shallow waters (80 m). At this station,  $D_{Fe}$  concentrations were remarkably high ( $>0.5\ nM$ ), with a  $2.16\ nM$  peak at 50 m depth and surface values were close to  $1\ nM$  (Fig. 6A). Interestingly, Chl *a* concentration within this mixed, and potentially

turbid, water column were low, with a mean value of  $0.5\ \mu g\ L^{-1}$ , suggesting the potential for light limitation within near-shore waters.

Station 568, is located northeast of 567 and at  $\sim 8.2\ km$  distance from the shore. Within the mixed layer (80 m),  $D_{Fe}$  and Chl *a* concentrations were relatively constant, at around  $0.5\ nM$  and  $0.5\ \mu g\ L^{-1}$ , respectively. Elevated  $D_{Fe}$  concentrations of  $1\ nM$  at 200 m then  $2\ nM$  at 300 m, and a lower value of  $0.5\ nM$  near the bottom (376 m) were observed. The last station (569) offshore in this transect was located 16 km away from the shore. Here again, within the mixed layer (50 m)  $D_{Fe}$  and Chl *a* were relatively constant. An increase in the  $D_{Fe}$  concentration of  $0.4\ nM$  was observed at 300 m depth. Chl *a* concentration were higher at Station 569, up to  $1.67\ \mu g\ L^{-1}$ , which corresponded to a low  $D_{Fe}$  concentration ( $0.18\ nM$ ) in surface waters.

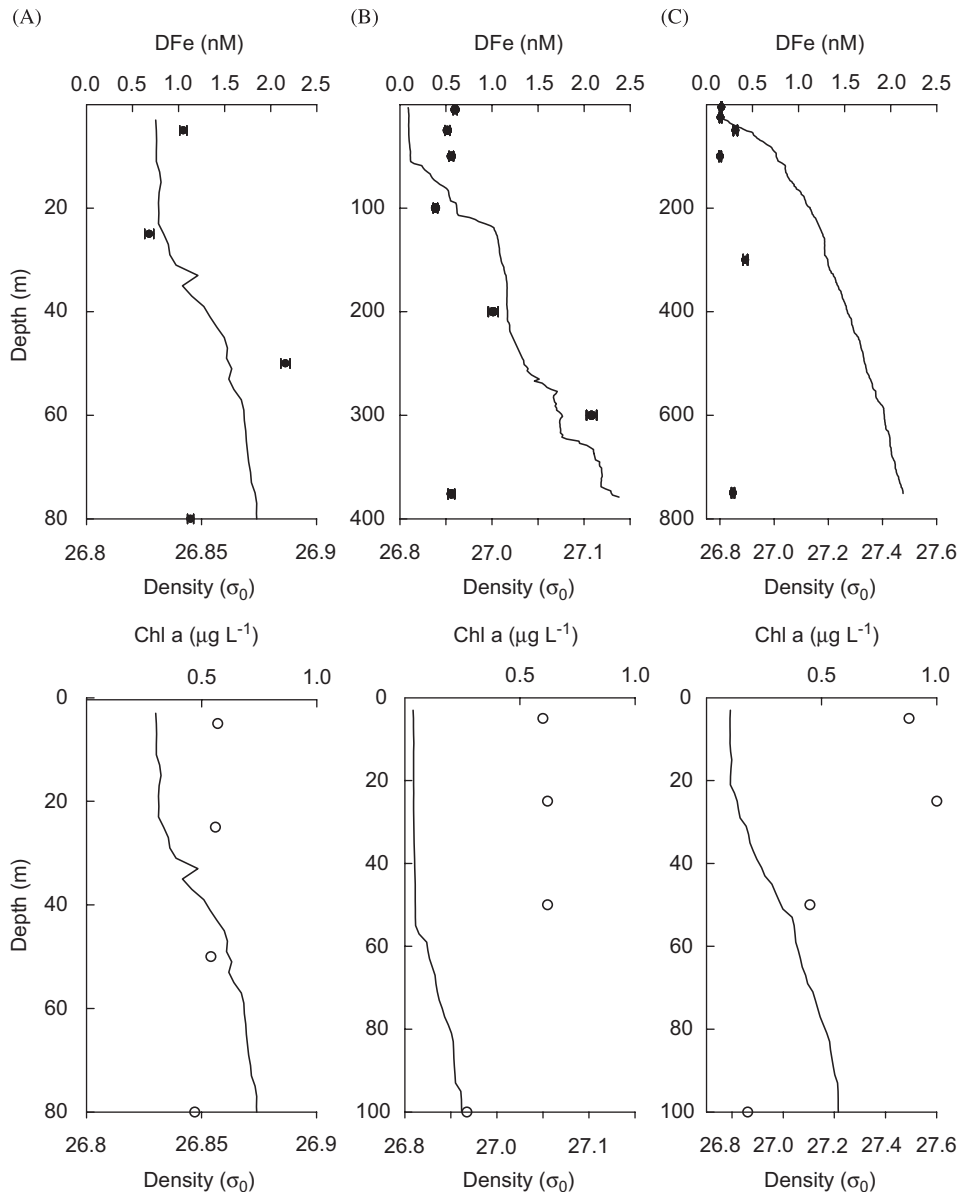


Fig. 6. Water column profiles of  $D_{Fe}$ , salinity, temperature and Chlorophyll  $a$  along a transect from Baie Américaine on 22/12/2004: (A) BA, Station 567; (B) BA + 1, Station 568 and (C) BA + 2, Station 569.

### 3.3.4. Other stations: M1 (491), M10 (563), M7 (524)

Vertical profiles (Table 1) obtained downstream of the islands (Stations M1, M10, M7) exhibit similar concentrations to those reported by Croot et al. (2004a) and Sedwick et al. (2002) for the 0.4- $\mu\text{m}$  filtered fraction, with concentrations ranging from 0.1 nM in surface waters to 0.5 nM at greater depths. A low-level variability is evident between

these stations, with concentrations ranging from 0.2 to 0.4 nM in the upper water column.

M1 and M7 were sampled in November; when the concentrations of Chl  $a$  were quite high for both, 0.79 for M1 and up to  $1.20 \mu\text{g m}^{-3}$  at M7, respectively.  $D_{Fe}$  concentrations were very similar, around 0.3 nM in the upper water column with no depth related trends evident. M10 was sampled after the major blooms in late December. Concentrations

of Fe are higher, around 0.5 nM, and chlorophyll concentrations are very low,  $0.3 \mu\text{g L}^{-1}$ .

#### 4. Discussion

Examining the supply of Fe and the mechanisms that drive the annual phytoplankton bloom north of the Crozet Plateau are of great interest for understanding how natural Fe fertilization may alleviate HNLC conditions normally associated with the Southern Ocean. The present study will discuss briefly the relationship between Chl *a* and  $D_{\text{Fe}}$  distribution then focus on the relative importance of atmospheric, lateral and upwelling mixing processes in the supply of  $D_{\text{Fe}}$  to surface waters by using a variety of approaches.

##### 4.1. Upper water column (50 m) distributions of $D_{\text{Fe}}$ and their relationship to Chl *a*

Overall, the surface concentrations of  $D_{\text{Fe}}$  are similar to recently reported values in this sector of the Southern Ocean. Conducted in the late summer 1998, Croot et al. (2004a) using chemiluminescence detection found dissolved Fe ( $<0.4 \mu\text{m}$ ) concentrations from 0.04 to 0.58 nM along a  $6^\circ\text{E}$  transect. Sedwick et al. (2002), during ANTARES IV (January–February 1999) around the Crozet Islands, reported  $D_{\text{Fe}}$  concentrations varying between 0.09 and 0.50 nM over the top 300 m ( $<0.4 \mu\text{m}$ ) using catalytic spectrophotometric detection (Measures

et al., 1995). More recently, Blain et al. (2007) reported a mean concentration around the Kerguelen Islands of  $0.09 \pm 0.034 \text{ nM}$  over the top 500 m.

However, a study conducted around the Kerguelen Islands (Bucciarelli et al., 2001) observed considerably higher concentrations of  $D_{\text{Fe}}$ , in the order of 7 nM. This difference may be explained by the time of sampling, which was prior to the bloom event in October, therefore prior to the main uptake by the phytoplankton, as well as there being a high concentration of lithogenic material (Blain et al., 2001). As Fe is considered to be the main limiting nutrient, one might expect that a high input of Fe will promote a bloom, which will cause an increase in chlorophyll and gradually a decrease in Fe concentrations. However, we do not expect a simple relationship between  $D_{\text{Fe}}$  and Chl *a*. This may reflect changes in Fe uptake and the fact that the phytoplankton community is affected by other factors such as light availability and grazing (Lancelot et al., 2000). For example, the fact that the Chl *a* concentrations are low very close distance to the shore (Station 567) and where  $D_{\text{Fe}}$  are the highest could indicate that the light mixing regime is not favourable to the phytoplankton community in these likely turbid waters.

Repeated occupations of Station M3 provide a quasi time series and highlight the complexity of the processes influencing the bloom which is occasionally influenced by advection of near-surface waters from the south (Pollard et al., 2007). Fig. 7

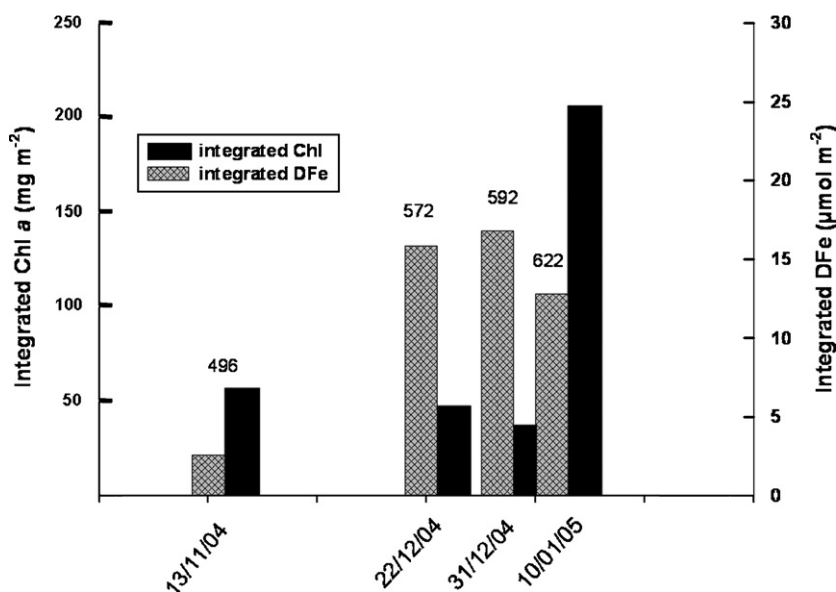


Fig. 7. Variation of integrated Chl *a* and  $D_{\text{Fe}}$  at Station M3.

represents the variation of integrated Chl *a* and  $D_{\text{Fe}}$  over time at M3. The first occupation of this Station (572) was sampled at the end of the main bloom, when biological uptake has probably reduced the bioavailable  $D_{\text{Fe}}$  to a concentration resulting in limitation of the phytoplankton population by mid-November. A temporally and spatially variable Fe resupply proximal to the Plateau may have occurred and reinitiated or maintained small bloom regions. It is also likely that some  $D_{\text{Fe}}$  recycling processes occur. A combination of these factors may thus explain the high-integrated Chl *a* observed in mid-January and simultaneous decrease in integrated  $D_{\text{Fe}}$  (Station 622). An additional factor of importance seems to be the ambient irradiance, which appeared to control the bloom initiation and early development (Venables et al., 2007).

Another approach to the link between primary production and  $D_{\text{Fe}}$  that has been taken by Moore et al. (2007a, b) is to calculate growth rates on addition of  $D_{\text{Fe}}$ . The reported values to the north of the plateau were of comparable magnitudes to estimates of maximal growth rates for natural population around the Kerguelen Islands (Blain et al., 2001). They also present evidence for Fe limitation within declining stages of the bloom to the north of the islands. Some relationships between enhanced phytoplankton photochemical efficiencies ( $F_v/F_m$ ) and higher  $D_{\text{Fe}}$  were also observed *in situ*. At any particular time the relationship between  $D_{\text{Fe}}$  and Chl *a* will also depend on the stage of bloom progression and the amount of biological Fe uptake that has occurred.

#### 4.2. Sources of dissolved iron

In the following section using the data available, estimates of the various sources of Fe to surface waters around the Crozet Islands and their relative importance are investigated.

##### 4.2.1. Atmospheric inputs

Model estimates based on composites of dust models (Jickells et al., 2005; Mahowald et al., 2005) give annual dust fluxes (wet and dry) of  $0.2 \text{ g m}^{-2} \text{ yr}^{-1}$  in this region, which corresponds to total Fe deposition, assuming an Fe content 3.5% (Jickells and Spokes, 2001) of  $132 \mu\text{mol m}^{-2} \text{ yr}^{-1}$ . There are limited data available for model calibration in the Southern Ocean region and many caveats associated with the aerosol and rainwater calculations (see Section 3.2). However, the two separate

approaches (model and field sampling) agree within a factor of three, lending confidence to the estimates. Model estimates suggest little seasonality in dust deposition, although fluxes are lower than the average by about a factor of 2 in the period March–June. During the phytoplankton productive season fluxes are similar to the annual average.

To estimate soluble Fe inputs we used our field data (Section 3.2) and assumed a solubility for dry deposition of 8% (Baker et al., 2006b) and 14% for wet deposition (Jickells and Spokes, 2001), yielding a soluble Fe input of  $38 \mu\text{mol m}^{-2} \text{ yr}^{-1}$ , equivalent to a dissolved Fe flux ( $F_{\text{atm}}$ ) of 104 (rounded to 100)  $\text{nmol m}^{-2} \text{ d}^{-1}$  (Fig. 9). Since the review by Jickells and Spokes (2001), Willey et al. (2004) and Kieber et al. (2005) have reported the active photochemical production of soluble Fe(II) and also higher Fe solubilities in North Atlantic rains, while Halstead et al. (2000) report similar solubilities to those of Jickells and Spokes (2001). The solubility of Fe in rainwater is clearly an important uncertainty in these calculations and merits further study.

It is not straightforward to estimate uncertainties on the overall soluble Fe flux presented in Table 4. This uncertainty will have three main components—physical flux (precipitation/deposition velocity), concentration variation and solubility, plus analytical uncertainties that are generally small by comparison. Deposition velocities are considered to have an uncertainty of a factor of 3 (Duce et al., 1991), and our estimate of rainfall amount in 3.2 has a 50% uncertainty. The overall variability of aerosol concentrations is 25–100% (Table 4) among the suite of samples we collected, but of course this set is from a limited field campaign and it is unlikely we captured the full range of variability seen in this area. Our rainwater concentrations have been volume-weighted, which provides a more reliable average but means we cannot directly provide an estimate of variability. Since total soluble Fe fluxes are dominated by wet deposition, the uncertainties in precipitation amount (factor of 2), volume weighted concentration and solubility dominate. Thus it seems likely that the uncertainty in fluxes is of the order of a factor 2–5. Mahowald et al. (2005) suggest uncertainties in model based dust fluxes are probably an order of magnitude.

##### 4.2.2. Vertical transport of $D_{\text{Fe}}$ to surface water

Charette et al. (2007) used a simple one-dimensional diffusive model on the vertical profile of

$^{228}\text{Ra}$  at M3 along with an average dissolved Fe gradient across the same depth interval, and determined two mixing scenarios: a slow mixing situation between 1000 and 300 m depth ( $K_z = 1.5 \text{ cm}^2 \text{ s}^{-1}$ ) and a fast mixing situation between 5 and 300 m depth ( $K_z = 11 \text{ cm}^2 \text{ s}^{-1}$ ). The maximum contribution of this potential source is then obtained using the upper estimate of the mixing rate ( $11 \text{ cm}^2 \text{ s}^{-1}$ ) over the top 300 m and a  $D_{\text{Fe}}$  gradient of  $0.64 \text{ nmol m}^{-3} \text{ m}^{-1}$  (0.15 nM at 5 m depth, 0.34 nM at 300 m) and the maximum  $D_{\text{Fe}}$  vertical mixing rate would be  $F_z = 61 \text{ nmol m}^{-2} \text{ d}^{-1}$  (Fig. 9). Blain et al. (2007) reported a  $K_z$  of  $3.3 \text{ cm}^2 \text{ s}^{-1}$  over the Kerguelen Plateau, leading to a vertical input of  $31 \text{ nmol m}^{-2} \text{ d}^{-1}$ .

#### 4.2.3. Lateral sources of Fe from the island system

The last input one can consider in this system with the data available is the lateral transport of dissolved Fe from the islands to the surrounding waters.

The average water-column  $D_{\text{Fe}}$  concentrations found immediately in the vicinity of Baie Américaine are 1.25 nM at Station 567 (closest to the islands) and 0.81 nM at Station 568. These are the highest concentrations found during our study and give us reasonable confidence that the island system is a source of Fe. This source can be from sediments on the shelf (Elrod et al., 2004), direct runoff, and

there is also the possibility that soluble Fe can be leached from suspended particles as they are laterally advected through the water column (Lam et al., 2006).

Moreover, Stations 567, 568, 569 (Baie Américaine) and 572 (M3) show a clear decreasing gradient (Fig. 8) of  $D_{\text{Fe}}$  concentrations at all depths. Using the same approach as Johnson et al. (1997), it is possible to estimate a scale length, which is defined as “the distance over which concentrations drop to  $1/e$  of the initial value”. Looking at the upper 50 m, our scale length is 25 km, which is considerably lower than the scale length of 151 km estimated by Bucciarelli et al. (2001) in the vicinity of Kerguelen Islands in the near-shore waters. This difference may be explained by a different circulation pattern around the two islands but more importantly by the difference between the respective surface areas of the islands. The Kerguelen Islands have a surface area of  $7000 \text{ km}^2$  and the Crozet Islands only  $350 \text{ km}^2$ ; thus the magnitude of natural Fe fertilization could be lowered. Significant loss of horizontally advected Fe from the sediments and shelf can occur too, in particular with scavenging onto sinking particles before all of this Fe can be distributed to the entire bloom region, which extends well north of M3.

The circulation as described by Pollard et al. (2007) has the consequence of semi-enclose the area

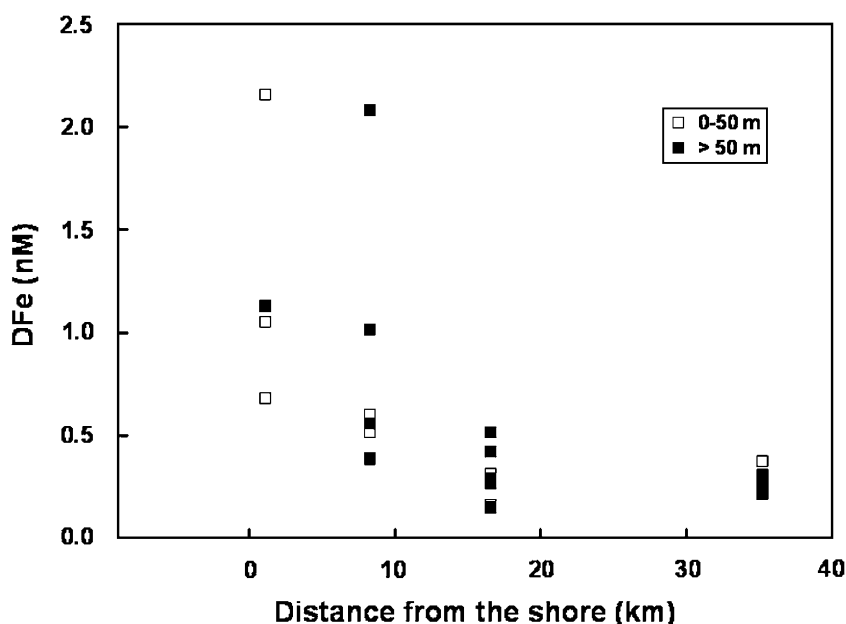


Fig. 8.  $D_{\text{Fe}}$  versus distance from the shore along the Baie Américaine transect extended out to M3 (Station 572).



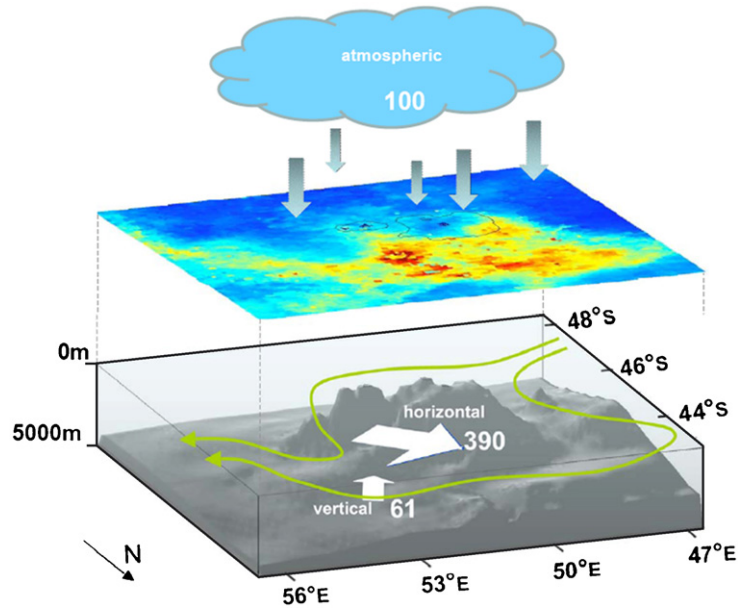


Fig. 9. Main pathways of  $D_{Fe}$  in  $\text{nmol m}^{-2} \text{d}^{-1}$  into the bloom area around the Crozet Islands combining the main circulation paths (green lines), topography and a SeaWiFS chlorophyll a image for the austral summer 2004–2005.

to the north of the Crozet Plateau (Fig. 3), where the residence time of surface water is  $\sim 60$  days. Consequently the large bloom observed in this HNLC area is clearly constrained by this northern branch, as well as any dissolved Fe from the islands and the associated plateau.

If one considers the island and the plateau systems to be a source of Fe throughout the year, then during the low light conditions of the winter when primary production is low, the concentration of Fe can build up and disperse laterally and then be readily available in springtime. Charette et al. (2007) used short-lived Radium isotopes  $^{223}\text{Ra}$  and  $^{224}\text{Ra}$  on the transect from Baie Américaine (Stations 567, 568 and 569) to provide an upper estimate of this horizontal flux ( $F_h$ ) of  $236 \mu\text{mol m}^{-2} \text{d}^{-1}$  using a linear gradient of  $0.07 \text{ nM km}^{-1}$  (average of  $D_{Fe}$  in the upper 50 m). Giret et al. (2002) reported a homogeneous mantle geochemical composition in this zone, so it seems reasonable to assume that the two main islands are geochemically representative of the Archipelago and that the offshore gradient will be representative of the islands and shelf system as a whole.

Using a 600-km shoreline and a bloom area of  $90,000 \text{ km}^2$  (Charette et al., 2007), the cumulative effect of this horizontal flux is estimated to be up to  $390 \text{ nmol m}^{-2} \text{d}^{-1}$ , which is considerably higher than either the atmospheric or vertical inputs

(Fig. 9). Another important fact is that the horizontal gradient of  $D_{Fe}$  was calculated in the upper 50 m near the shore therefore not including the deeper waters nor the plateau itself. This  $D_{Fe}$  gradient would be enhanced further if the whole width of the continental shelf is considered (Luther and Wu, 1997).

#### 4.3. Estimation of $D_{Fe}$ before the main bloom event

To constrain the potential of an island Fe source initiating the austral spring bloom, it is possible to estimate the  $D_{Fe}$  concentration that would have built up over the Austral winter.

This region under the island effect can be subjected to the three types of inputs that have been considered in this work: atmospheric, vertical and horizontal fluxes. The addition of these three fluxes multiplied by a winter period of 100 days, and over a winter mixed-layer depth of 100 m (Eq. (4)), leads to a final concentration of  $D_{Fe}$  prior to the bloom of  $0.55 \text{ nM}$ :

$$\frac{(F_{\text{atm}} + F_z + F_h) \times 100}{100} \quad (4)$$

This estimate is lower than but of the same magnitude as the  $0.75 \text{ nM}$  demand derived independently by Lucas et al. (2007). Overall our calculations support the view that our  $D_{Fe}$  fluxes can

support phytoplankton new production in the northern bloom region, but only by invoking  $D_{\text{Fe}}:\text{N}$  cell quotas of  $<0.06 \text{ mmol mol}^{-1}$  (Lucas et al., 2007), which probably reflects the relative availability of ambient  $D_{\text{Fe}}$  and N.

In addition to Fe sources so far discussed, it is also important to look at the potential role of suspended particles. Soluble Fe can be leached from suspended particles as they are laterally advected through the water column, as recently described by Lam et al. (2006). It is also possible that colloidal Fe may be released from sediments and added to Fe advected to the bloom area. These additional sources could increase the Fe budget at the end of the winter and require further investigation.

## 5. Summary and conclusions

The area investigated by CROZEX covers a broad range of hydrographic and biogeochemical conditions and therefore allows a comparison between a low-productivity low-Fe zone and a high-productivity, relatively high-Fe zone at the edge of the Southern Ocean. Overall, the concentrations of  $D_{\text{Fe}}$  found are low in surface waters because we sampled after the main bloom event, and they are in the range of values reported in other studies from this area (Sedwick et al., 2002. Croot et al., 2004a).

This data set allows us to propose a scenario for the bloom initiation and maintenance northwards of the Crozet Archipelago during the austral summer. The transect of stations from Baie Américaine shows a distinct concentration gradient, thus providing strong evidence for the island shelf system being a source of Fe. Other input terms to the surface water considered included atmospheric deposition input and vertical mixing. However, the present estimate shows that horizontal advection is the largest term, followed by the atmospheric and then the vertical mixing. Over the winter period when productivity is light limited, the concentration of Fe is estimated to build up to  $\sim 0.55 \text{ nM}$  in waters to the north of the islands. As light levels increase gradually over the spring and summer, the bloom can be initiated and progress with this ambient  $D_{\text{Fe}}$ .

This first overall estimate of Fe supply fuelling the bloom to the north of the Crozet Islands therefore provides a rationalization and an indication of the relative importance of different sources of Fe in these Sub-Antarctic Island systems. Present significant uncertainties include the recycling and removal

of Fe and the significance and availability of particulate Fe to the primary producers.

## Acknowledgments

We would like to thank the Captain, officers, engineers, technicians and crew of the *RRS Discovery* for their enthusiasm and their professional assistance. These cruises were the two first of the Crozex project, which was a contribution to a British BICEP (Biophysical Interactions and Control of Export Production)—NERC program. This work was also supported by NERC Grant NE/B502844/1 and a NERC Ph.D. studentship for M.F.

We also acknowledge R. Pollard and E. Popova for their help with illustrations, and the thoughtful and constructive comments of three anonymous referees who greatly improved the quality of this paper.

## References

- Arrigo, K.R., Worthen, D., Schnell, A., Lizotte, M.P., 1998. Primary production in Southern Ocean waters. *Journal of Geophysical Research* 103 (C8), 15,587–15,600.
- De Baar, H.J.W., de Jong, J.T.M., Nolting, R.F., van Leeuwe, M.A., Timmermans, K.R., Templin, M., Rutgers van der Loeff, M.M., Sildam, J., 1999. Low dissolved Fe and the absence of diatom blooms in remote Pacific waters of the Southern Ocean. *Marine Chemistry* 66, 1–34.
- De Baar, H.J.W., Boyd, P.W., Coale, K.H., Landry, M.R., Tsuda, A., Assmy, P., Bakker, D.C.E., Bozec, Y., Barber, R.T., Brzezinski, M.A., Buesseler, K.O., Boyé, M., Croot, P.L., Gervais, F., Gorbunov, M.Y., Harrison, P.J., Hiscock, W.T., Laan, P., Lancelot, C., Law, C.S., Levasseur, M., Marchetti, A., Millero, F.J., Nishioka, J., Nojiri, Y., van Oijen, T., Riebesell, U., Rijkenberg, M.J.A., Saito, H., Takeda, S., Timmermans, K.R., Veldhuis, M.J.W., Waite, A., Wong, C.S., 2005. Synthesis of iron fertilization experiments: from the Iron Age in the age of enlightenment. *Journal of Geophysical Research (Oceans)* 110 (C09S16), 1–24.
- Baker, A.R., Kelly, S.D., Biswas, K.F., Witt, M., Jickells, T.D., 2003. Atmospheric deposition of nutrients to the Atlantic Ocean. *Geophysical Research Letters* 30, 2296.
- Baker, A.R., French, M., Linge, K.L., 2006a. Trends in aerosol nutrient solubility along a west-east transect of the Saharan dust plume. *Geophysical Research Letters* 33, L07805.
- Baker, A.R., Jickells, T.D., Witt, M., Linge, K.L., 2006b. Trends in the solubility of iron, aluminium, manganese and phosphorus in aerosol collected over the Atlantic Ocean. *Marine Chemistry* 98, 43–58.
- Bakker, D.C.E., Watson, A.J., Law, C.S., 2001. Southern Ocean iron enrichment promotes inorganic carbon drawdown. *Deep-Sea Research II* 48, 2483–2507.
- Bakker, D.C.E., Bozec, Y., Nightingale, P.D., Goldson, L., Messias, M.-J., De baar, H.J.W., Liddicoat, M., Skjelvan, I., Strass, V., Watson, A.J., 2005. Iron and mixing affect

- biological carbon uptake in SOIREE and EISENEX. Two Southern Ocean iron fertilisation experiments. *Deep-Sea Research I* 52, 1001–1019.
- Blain, S., Tréguer, P., Belviso, S., Bucciarelli, E., Denis, M., Desabre, S., Fiala, M., Martin Jézéquel, V., Le Fèvre, J., Mayzaud, P., Marty, J.-C., Razouls, S., 2001. A biogeochemical study of the island mass effect in the context of the iron hypothesis: Kerguelen Islands, Southern Ocean. *Deep-Sea Research I* 48 (1), 163–187.
- Blain, S., Sedwick, P.N., Griffiths, F.B., Quéguiner, B., Bucciarelli, E., Fiala, M., Pondaven, P., Tréguer, P., 2002. Quantification of algal iron requirements in the Subantarctic Southern Ocean (Indian sector). *Deep-Sea Research II* 49 (16), 3255–3273.
- Blain, S., Quéguiner, B., Armand, L., Belviso, S., Bomble, B., Bopp, L., Bowie, A., Brunet, C., Brussaard, C., Carlotti, F., Christaki, U., Corbière, A., Durand, I., Ebersbach, F., Fuda, J.-L., Garcia, N., Gerringa, L., Griffiths, B., Guigue, C., Guillemin, C., Jacquet, S., Jeandel, C., Laan, P., Lefèvre, D., Lo Monaco, C., Malits, A., Mosseri, J., Obernosterer, I., Park, Y.-H., Picheral, M., Pondaven, P., Remenyi, T., Sandroni, V., Sarthou, G., Savoye, N., Scouarnec, L., Souhaut, M., Thuiller, D., Timmermans, K., Trull, T., Uitz, J., van Beek, P., Veldhuis, M., Vincent, D., Viollier, E., Vong, L., Wagener, T., 2007. Effect of natural iron fertilization on carbon sequestration in the Southern Ocean. *Nature* 446, 1070–1074.
- Boyd, P.W., Watson, A.J., Law, C.S., Abraham, E.R., Trull, T., Murdoch, R., Bakker, D.C.E., Bowie, A.R., Buesseler, K.O., Chang, H., Charette, M., Croot, P., Downing, K., Frew, R., Gall, M., Hadfield, M., Hall, J., Harvey, M., Jameson, G., LaRoche, J., Liddicoat, M., Ling, R., Maldonado, M.T., McKay, R.M., Nodder, S., Pickmere, S., Pridmore, R., Rintoul, S., Safi, K., Sutton, P., Strzepek, R., Tanneberger, K., Turner, S., Waite, A., Zeldis, J., 2000. A mesoscale phytoplankton bloom in the polar Southern Ocean stimulated by iron fertilization. *Nature* 407, 695–702.
- Boyd, P.W., Law, C.S., Wong, C.S., Nojiri, Y., Tsuda, A., Levasseur, M., Takeda, S., Rivkin, R., Harrison, P.J., Strzepek, R., Gower, J., McKay, R.M., Abraham, E., Arychuk, M., Barwell-Clarke, J., Crawford, W., Crawford, D., Hale, M., Johnson, K., Kiyosawa, J., Kudo, I., Marchetti, A., Miller, W., Needoba, J., Nishioka, J., Ogawa, J., Page, J.T., Robert, M., Saito, H., Sastri, A., Sherry, N., Soutar, T., Sutherland, N., Taira, Y., Whitney, F., Wong, S.K.E., 2004. The decline and fate of an iron-induced Subarctic phytoplankton Bloom. *Nature* 428, 549–553.
- Boyd, P.W., Jickells, T., Law, C.S., Blain, S., Boyle, E.A., Buesseler, K.O., Coale, K.H., Cullen, J.J., de Baar, H.J.W., Follows, M., Harvey, M., Lancelot, C., Levasseur, M., Owens, N.P.J., Pollard, R., Rivkin, R.B., Sarmiento, J., Schoemann, V., Smetacek, V., Takeda, S., Tsuda, A., Turner, S., Watson, A.J., 2007. Mesoscale iron enrichment experiments 1993–2005: synthesis and future directions. *Science* 315, 612–617.
- Boyé, M., Nishioka, J., Croot, P.L., Laan, P., Timmermans, K.R., de Baar, H.J.W., 2005. Major deviations of iron complexation during 22 days of a mesoscale iron enrichment in the open Southern Ocean. *Marine Chemistry* 96 (3–4), 257–271.
- Bucciarelli, E., Blain, S., Tréguer, P., 2001. Iron and manganese in the wake of the Kerguelen Islands (Southern Ocean). *Marine Chemistry* 73 (1), 21–36.
- Buesseler, K.O., Andrews, J.E., Pike, S.M., Charette, M.A., 2004. The effects of iron fertilization on carbon sequestration in the Southern Ocean. *Science* 304, 414–417.
- Charette, M.A., Gonneea, M. E., Morris, P.J., Statham, P.J., Fones, G.R., Planquette, H.F., Salter, I., Naveira Garabato, A., 2007. Radium isotopes as tracers of iron sources fueling a Southern Ocean phytoplankton bloom. *Deep-Sea Research II*, this issue [doi:10.1016/j.dsr2.2007.06.003].
- Chisholm, S.W., 2000. Oceanography: stirring times in the Southern Ocean. *Nature* 407, 685–687.
- Coale, K.H., Johnson, K.S., Chavez, F.P., Buesseler, K.O., Barber, R.T., Brzezinski, M.A., Cochlan, W.P., Millero, F.J., Falkowski, P.G., Bauer, J.E., Wanninkhof, R.H., Kudela, R.M., Altabet, M.A., Hales, B.E., Takahashi, T., Landry, M.R., Bidigare, R.R., Wang, X., Chase, Z., Strutton, P.G., Friederich, G.E., Gorbunov, M.Y., Lance, V.P., Hiltling, K.A., Hiscock, M.R., Demarest, M., Hiscock, W.T., Sullivan, K.F., Tanner, S.J., Gordon, M.R., Hunter, C.N., Elrod, V.A., Fitzwater, S.E., Jones, J.L., Tozzi, S., Kobalick, M., Roberts, A.E., Herndon, J., Brewster, J., Ladizinsky, N., Smith, G., Cooper, D., Timothy, D., Brown, S.L., Selph, K.E., Sheridan, C.C., Twining, B.S., Johnson, Z.I., 2004. Southern Ocean iron enrichment experiment: carbon cycling in high- and low-Si waters. *Science* 304 (5669), 408–414.
- Croot, P.L., Andersson, K., Oztürk, M., Turner, D.R., 2004a. The distribution and speciation of iron along 60°E in the Southern Ocean. *Deep-Sea Research II* 51, 2857–2879.
- Croot, P.L., Streu, P., Baker, A.R., 2004b. Short residence time for iron in surface water impacted by atmospheric dry deposition from Saharan dust events. *Geophysical Research Letters* 31, L32S08.
- Croot, P.L., Laan, P., Nishioka, J., Boyé, M., Timmermans, K.R., Bellerby, R.G., Goldson, L., Nightingale, P., de Baar, H.J.W., 2005. Spatial and temporal distribution of Fe(II) and H<sub>2</sub>O<sub>2</sub> during EISENEX, an open ocean mesoscale iron enrichment. *Marine Chemistry* 95, 65–88.
- Draxler, R.R., Rolph, G.D., 2003. HYSPLIT (Hybrid Single-Particle Lagrangian Integrated Trajectory) Model access via NOAA ARL READY website <<http://www.arl.noaa.gov/ready/hysplit4.html>> NOAA Air Resources Laboratory, Silver Spring, MD.
- Duce, R.A., Liss, P.S., Merrill, J.T., Atlas, E.L., Buat-Ménard, P., Hicks, B.B., Miller, J.M., Prospero, J.M., Arimoto, R., Church, T.M., Ellis, W.E., Galloway, J.N., Hansen, L., Jickells, T.D., Knap, A.H., Reinhardt, K.H., Schneider, B., Soudine, A., Tokos, J.J., Tsunogai, S., Wollast, R., Zhou, M., 1991. The atmospheric input of trace species to the world ocean. *Global Biogeochemical Cycles* 5, 193–259.
- Elrod, V.A., Berelson, W.M., Coale, K.H., Johnson, K.S., 2004. The flux of iron from continental shelf sediments: a missing source for global budgets. *Geophysical Research Letter* 31, L12307, doi:10.1029/2004GLO20216.
- Fiala, M., Delille, B., Dubreuil, C., Kopczynska, E., Leblanc, K., Morvan, J., Quéguiner, B., Blain, S., Caillau, C., Conan, P., Corvaisier, R., Denis, M., Frankignoulle, M., Oriol, L., Roy, S., 2003. Mesoscale surface distribution of biogeochemical characteristics in the Crozet Basin frontal zones (South Indian Ocean). *Marine Ecology Progress Series* 249, 1–14.
- Gaiero, D.M., Probst, J.-L., Depetris, P.J., Bidart, S.M., Leleyter, L., 2003. Iron and other transition metals in Patagonian riverborne and windborne materials: geochemical

- control and transport to the Southern South Atlantic Ocean. *Geochimica et Cosmochimica Acta* 67 (19), 3603–3623.
- Giret, A., Tourpin, S., Marc, S., Verdier, O., Cottin, J.-Y., 2002. Volcanisme de l'île aux Pingouins, archipel Crozet, témoin de l'hétérogénéité du manteau fertile au sud de l'océan Indien. Penguins Island, Crozet archipelago, volcanic evidence for a heterogeneous mantle in the Southern Indian Ocean. *Comptes Rendus Geosciences* 334, 481–488.
- Halstead, M.J.R., Cunninghame, R.G., Hunter, K.A., 2000. Wet deposition of trace metals to a remote site in Fiordland, New Zealand. *Atmospheric Environment* 34 (4), 665–676.
- Jickells, T.D., An, Z.S., Andersen, K.K., Baker, A.R., Bergametti, G., Brooks, N., Cao, J.J., Boyd, P.W., Duce, R.A., Hunter, K.A., Kawahata, H., Kubilay, N., laRoche, J., Liss, P.S., Mahowald, N., Prospero, J.M., Ridgwell, A.J., Tegen, I., Torres, R., 2005. Global iron connections between desert dust, ocean biogeochemistry and climate. *Science* 308, 67–71.
- Jickells, T.D., Spokes, L.J., 2001. Atmospheric iron inputs to the Oceans. In: Turner, D.R., Hunter, K.A. (Eds.), *The Biogeochemistry of Iron in Seawater*. IUPAC Series on Analytical and Physical Chemistry of Environmental Systems. Wiley, Chichester, pp. 85–121.
- Johnson, K.S., Gordon, R.M., Coale, K.H., 1997. What controls dissolved iron concentrations in the world ocean? *Marine Chemistry* 57, 137–161.
- Jickells, T.D., Kelly, S.D., Baker, A.R., Biswas, K., Dennis, P.F., Spokes, L.J., Witt, M., Yeatman, S.G., 2003. Isotopic evidence for a marine ammonia source. *Geophysical Research Letters* 30 (7), 1374.
- De Jong, J.T.M., den Das, J., Bathmann, U., Stoll, M.H.C., Kattner, G., Nolting, R.F., de Baar, H.J.W., 1998. Dissolved iron at subnanomolar levels in the Southern Ocean as determined by shipboard analysis. *Analytica Chimica Acta* 377, 113–124.
- Kieber, R.J., Skrabal, S.A., Smith, B.J., Willey, J.D., 2005. Organic complexation of Fe(II) and its impact on the redox cycling of iron in rain. *Environmental Science and Technology* 39 (6), 1576–1583.
- Korb, R.E., Whitehouse, M.J., Ward, P., 2004. SeaWIFS in the Southern Ocean: spatial and temporal variability in phytoplankton biomass around South Georgia. *Deep-Sea Research II* 51 (1–3), 99–116.
- Lam, P.J., Bishop, J.K.B., Henning, C.C., Marcus, M.A., Waychunas, G.A., Fung, I.Y., 2006. Wintertime phytoplankton bloom in the Subarctic Pacific supported by continental margin iron. *Global Biogeochemical Cycles* 20 (1).
- Lancelot, C., Hannon, E., Becquevort, S., Veth, C., De Baar, H.J.W., 2000. Modeling phytoplankton blooms and carbon export production in the Southern Ocean: dominant controls by light and iron in the Atlantic sector in Austral spring 1992. *Deep-Sea Research I* 47 (9), 1621–1662.
- Luther, G.W., Wu, J., 1997. What controls dissolved iron concentrations in the world ocean?—A comment. *Marine Chemistry* 57, 173–179.
- Law, C.S., Crawford, W.R., Smith, M.J., Boyd, P.W., Wong, C.S., Nojiri, Y., Robert, M., Abraham, E.R., Johnson, W.K., Forsland, V., Arychuk, M., 2006. Patch evolution and the biogeochemical impact of entrainment during an iron fertilisation experiment in the sub-Arctic Pacific. *Deep-Sea Research II* 53, 2012–2033.
- Löscher, B.M., 1999. Relationships among Ni, Cu, Zn, and major nutrients in the Southern Ocean. *Marine Chemistry* 67, 67–102.
- Lohan, M.C., Aguilar-Islas, A., Bruland, K.W., 2006. Direct determination of iron in acidified (pH 1.7) seawater samples by flow injection analysis with catalytic spectrophotometric detection: application and intercomparison. *Limnology and Oceanography (Methods)* 4, 164–171.
- Lucas, M., Seeyave, S., Sanders, R., Moore, C.M.M., Williamson, R., Stinchcombe, M., 2007. Nitrogen uptake responses to a naturally Fe-fertilised phytoplankton bloom during the 2004/5 CROZEX study. *Deep-Sea Research*, this issue [doi:10.1016/j.dsr2.2007.06.017].
- Mahowald, N.M., Baker, A.R., Bergametti, G., Brooks, N., Jickells, T.D., Duce, R.A., Kubilay, N., Prospero, J.M., Tegen, I., 2005. The atmospheric global dust cycle and iron inputs to the ocean. *Global Biogeochemical Cycles* 19, GB4025.
- Martin, J.H., 1990. Glacial–interglacial CO<sub>2</sub> change: the iron hypothesis. *Paleoceanography* 5 (1), 1–13.
- Measures, C.I., Yuan, J., Resing, J.A., 1995. Determination of iron in seawater by flow injection analysis using in-line preconcentration and spectrophotometric detection. *Marine Chemistry* 50 (1–4), 3–12.
- Metzl, N., Tilbrook, B., Poisson, A., 1999. The annual fCO<sub>2</sub> cycle and the air–sea CO<sub>2</sub> flux in the sub-Antarctic Ocean. *Tellus* 51B, 849–861.
- Moore, C.M.M., Seeyave, S., Hickman, A.E., Allen, J.T., Lucas, M.I., Planquette, H., Pollard, R.T., Poulton A.J., 2007a. Iron-light interactions during the CROZet natural iron bloom and EXport experiment (CROZEX) I: phytoplankton growth and photophysiology. *Deep-Sea Research (II)*, this issue [doi:10.1016/j.dsr2.2007.06.011].
- Moore, C.M.M., Hickman, A.E., Poulton, A.J., Seeyave, S., Lucas, M.I., 2007b. Iron-light interactions during the CROZet natural iron bloom and EXport experiment (CROZEX) II: taxonomic responses and elemental stoichiometry. *Deep-Sea Research (II)*, this issue [doi:10.1016/j.dsr2.2007.06.015].
- Moore, J.K., Abbott, M.R., 2002. Surface chlorophyll concentrations in relation to the Antarctic Polar Front: seasonal and spatial patterns from satellite observations. *Journal of Marine Systems* 37, 69–86.
- Park, Y.-H., Pollard, R.T., Read, J.F., Lebourcier, V., 2002. A quasi-synoptic view of the frontal circulation in the Crozet Basin during the Antares-4 cruise. *Deep-Sea Research II* 49 (9–10), 1823–1842.
- Pollard, R.T., Read, J.F., 2001. Circulation pathways and transports of the Southern Ocean in the vicinity of the Southwest Indian Ridge. *Journal of Geophysical Research* 106 (C2), 2881–2898.
- Pollard, R.T., Lucas, M.I., Read, J.F., 2002. Physical controls on biogeochemical zonation in the Southern Ocean. *Deep-Sea Research Part II—Topical Studies in Oceanography* 49 (16), 3289–3305.
- Pollard, R.T., Venables, H.J., Read, J.F., Allen, J.T., 2007. Large scale circulation around the Crozet Plateau controls an annual phytoplankton bloom in the Crozet Basin. *Deep-Sea Research II*, this issue [doi:10.1016/j.dsr2.2007.06.012].
- Read, J.F., Pollard, R.T., Allen, J.T., 2007. Sub-mesoscale structure and the development of an eddy in the Subantarctic Front north of Crozet Islands. *Deep-sea Research II*, this issue [doi:10.1016/j.dsr2.2007.06.013].
- Sanders, R., Morris, P.J., Stinchcombe, M., Seeyave, S., Venables, H.J., Lucas, M.I., 2007. New production and the

- f-ratio around the Crozet Plateau in austral summer 2004-5 diagnosed from seasonal changes in inorganic nutrient levels. *Deep-Sea Research II*, this issue [doi:10.1016/j.dsr2.2007.06.007].
- Sarmiento, J.L., Hughes, T.M.C., Stouffer, R.J., Manabe, S., 1998. Simulated response of the ocean carbon cycle to anthropogenic climate warming. *Nature* 393 (6682), 245–249.
- Sarthou, G., Jeandel, C., Brisset, L., Amouroux, D., Besson, T., Donard, O.F.X., 1997. Fe and H<sub>2</sub>O<sub>2</sub> distributions in the upper water column in the Indian sector of the Southern Ocean. *Earth and Planetary Science Letters* 147, 83–92.
- Sarthou, G., Baker, A.R., Blain, S., Achterberg, E.P., Boyé, M., Bowie, A.R., Croot, P.L., Laan, P., de Baar, H.J.W., Jickells, T.D., Worsfold, P., 2003. Atmospheric iron deposition and sea-surface dissolved iron concentrations in the eastern Atlantic Ocean. *Deep-Sea Research I* 50 (10–11), 1339–1352.
- Sedwick, P.N., Blain, S., Quéguiner, B., Griffiths, F.B., Fiala, M., Bucciarelli, E., Denis, M., 2002. Resource limitation of phytoplankton growth in the Crozet Basin, Subantarctic Southern Ocean. *Deep-Sea Research Part II* 49 (16), 3327–3349.
- Seeyave, S., Lucas, M.I., Moore, C.M., Poulton, A.J., 2007. Phytoplankton productivity and community structure across the Crozet Plateau during summer 2004/2005. *Deep-Sea Research*, this issue [doi:10.1016/j.dsr2.2007.06.010].
- Spokes, L., Jickells, T.D., Jarvis, K., 2001. Atmospheric inputs of trace metals to the northeast Atlantic Ocean: the importance of southeasterly flow. *Marine Chemistry* 76, 319–330.
- Sunda, W.G., Huntsman, S.A., 1995. Iron uptake and growth limitation in oceanic and coastal phytoplankton. *Marine Chemistry* 50 (1–4), 189–206.
- Sunda, W.G., Huntsman, S.A., 1997. Interrelated influence of iron, light and cell size on marine phytoplankton growth. *Nature* 390, 389–392.
- Taljaard, J.J., Loom, H.V., 1984. Climatology of the Indian Ocean south of 35°S. In: Loom, H.V. (Ed.), *Climate of the Ocean*. Elsevier, Amsterdam, pp. 505–601, 716pp.
- Tréguer, P., Jacques, G., 1992. Dynamics of nutrient and phytoplankton and cycles of carbon, nitrogen and silicon in the Southern Ocean: a review. *Polar Biology* 12, 149–162.
- Tréguer, P., Pondaven, P., 2001. Preface: climatic changes and the carbon cycles in the Southern Ocean: a step forward. *Deep-Sea Research II* 49, 1597–1600.
- Venables, H., Pollard, R.T., Popova, E.E., 2007. Physical conditions controlling the early development of a regular phytoplankton bloom north of the Crozet Plateau, Southern Ocean. *Deep-Sea Research II*, this issue [doi:10.1016/j.dsr2.2007.06.014].
- Welschmeyer, N.A., 1994. Fluorometric analysis of chlorophyll-a in the presence of chlorophyll-b and pheopigments. *Limnology and Oceanography* 39 (8), 1985–1992.
- Willey, J.D., Kieber, R.J., Avery Jr., G.B., 2004. Effects of rainwater iron and hydrogen peroxide on iron speciation and phytoplankton growth in seawater near Bermuda. *Journal of Atmospheric Chemistry* 47 (3), 209–222.